A nonlinear finite volume scheme satisfying maximum and minimum principles for diffusion operators

Christophe Le Potier

▶ **To cite this version:**

Christophe Le Potier. A nonlinear finite volume scheme satisfying maximum and minimum principles for diffusion operators. International Journal on Finite Volumes, 2009, pp.1-20. hal-01116968

HAL Id: hal-01116968
https://hal.science/hal-01116968

Submitted on 16 Feb 2015

HAL is a multi-disciplinary open access archive for the deposit and dissemination of scientific research documents, whether they are published or not. The documents may come from teaching and research institutions in France or abroad, or from public or private research centers.

L'archive ouverte pluridisciplinaire **HAL**, est destinée au dépôt et à la diffusion de documents scientifiques de niveau recherche, publiés ou non, émanant des établissements d'enseignement et de recherche français ou étrangers, des laboratoires publics ou privés.

A nonlinear finite volume scheme satisfying maximum and minimum principles for diffusion operators

Christophe Le Potier
CEA, DEN, DM2S, SFME, F-91191 Gif-sur-Yvette, France.
clepotier@cea.fr

Abstract

We introduce a new finite volume method for highly anisotropic diffusion operators on triangular cells. The main idea is to calculate the gradient using a nonlinear scheme. For parabolic problems, the resulting global matrix is a strictly diagonally dominant M-Matrix without geometrical constraints on the mesh and restrictive conditions on the anisotropy ratio. We verify the accuracy of the method by comparing our computed solutions with analytical solutions. The efficiency of the algorithm is demonstrated by comparing it with numerical schemes which do not satisfy discrete minimum and maximum principles.

Key words : Finite Volumes, Maximum Principle, Anisotropic Diffusion

1 Introduction

In the framework of nuclear waste disposal simulation, we are interested in a transport model in porous media which can be described by a convection-diffusion-dispersion equation applied on highly anisotropic heterogeneous geological layers. For the convective term, we use a classical upwind scheme where the physical phenomenon is convection dominated, and a centered scheme where the physical phenomenon is diffusion dominated. The key property of this convection scheme is that it satisfies maximum and minimum principles. Therefore, it is natural to seek an approximation to the diffusive-dispersive term which has also these properties.

We are interested in constructing a cell-centered scheme which satisfies the following :

- it is second order accurate for smooth solutions.
- it takes into account heterogeneous anisotropic tensors.
- it takes into account distorted meshes.

- it satisfies discrete minimum and maximum principles (DMMP) without geometric constraints on the mesh and without conditions on the anisotropy ratio.

The crucial property is the fourth property. It is very important for diffusion terms in modelling two-phase flows in porous media [NOR 05] and for coupling transport equation with a chemical model.
To our knowledge, there are no linear schemes satisfying all of the above requirements. For example, for classical finite elements, it is explained in [CIA 73, KOR 00], that for the Laplacian, the resulting global matrix associated with the scheme is an M-Matrix if some geometrical constraints are satisfied. We can also cite a recent work described in [LP 09] where a linear scheme satisfying a maximum principle for anisotropic diffusion operators on distorted grids is developed. This method is generally first order accurate for smooth solutions.
However, a few non-linear methods have been proposed. In [BUR 04], a non linear correction of a finite linear element scheme is developed. But, heterogeneous anisotropic tensors are not taken into account. In [BER 06], an interesting non-linear method is proposed for homogeneous isotropic diffusion. Unfortunately, the positivity properties are obtained under restrictive geometric constraints. In [LP 05b], we proposed a cell-centered finite volume discretization for the diffusion operator. We showed the robustness and the accuracy of this algorithm in comparison with analytical solutions. This scheme satisfies either the minimum or the maximum principle but not the both simultaneously. This was extended in [KAP 07, LIP 07, LIP 09, YUA 08] on polygonal meshes and tetrahedrons.
In this paper, we construct a new algorithm which satisfies DMMP for any anisotropic tensor on unstructured triangular cells.
The outline of the paper is as follows. After a short presentation, we describe in subsection 2.1 the case where the diffusion tensor is equal to the identity matrix. Then, in subsection 2.2, we extend the algorithm to the heterogeneous anisotropic case. In section 3, we present a few numerical results and we conclude in section 4.

2 Presentation

Let Ω be an open bounded convex subset of $\mathcal{R}^2$. We consider the following problem

$$\left\{ \begin{array}{l} \vec{q} = \overline{\overline{D}} \vec{\nabla} C \\ \omega \dfrac{\partial C}{\partial t} = div\vec{q} \text{ on } \Omega \ \forall \text{t} > 0 \end{array} \right. \tag{1}$$

with

- ω, the porosity
- C, the radioactive element concentration
- $\overline{\overline{D}}$, a symmetric definite positive matrix

We also impose an initial condition and Dirichlet boundary conditions.

2.1 Isotropic homogeneous case: $\overline{\overline{D}} = Id$

We consider a grid $\mathcal{T}$ made up of N_{ma} triangular cells and N_f boundary edges. We define $\mathcal{B} = \{X_{j_{\{1\leq j\leq N_{ma}+N_f\}}}\}$ as the set of the points which are the intersection of the angle bisectors of each triangular cell and the points located at the midpoints of the edges of the boundary. For any node O_i of the grid (not located on the boundary), there exists a triangular cell $(X_{T_{i,1}}, X_{T_{i,2}}, X_{T_{i,3}})$ (with $X_{T_{i,j_{j=1,2,3}}} \in \mathcal{B}$) so that the node O_i is inside this triangular cell.
Remark 1: as Ω is convex, this triangular cell always exists. It is sufficient to take the triangular cells with vertices located at the midpoints of the edges of the boundary. In practice, we choose the points closest to O_i. So, there exists three positive or zero coefficients $\lambda_{i,j;j=1,2,3}$ with $\sum_{\{1\leq j\leq 3\}}\lambda_{i,j} = 1$ (Figure 1), such that $\sum_{\{1\leq j\leq 3\}}\lambda_{i,j}O_i\vec{X}_{T_{i,j}} = \vec{0}$.
Remark 2: several triangular cells can exist that satisfy the desired property. So, we can introduce several points $X_{T_{i,j},j=1,..,N}$ and $\lambda_{i,j;j=1,..,N}$ (with $N > 3$) such that $\sum_{\{1\leq j\leq N\}}\lambda_{i,j}O_i\vec{X}_{T_{i,j}} = \vec{0}$.
Remark 3: an other solution consists in integrating $div\vec{\nabla}x = 0$ and $div\vec{\nabla}y = 0$ on a disk around the node O_i. We obtain: $\sum_{\{j\in V_{O_i}\}}\lambda_{i,j}O_i\vec{X}_{T_{i,j}} = \vec{0}$ with $\lambda_{i,j} \geq 0$, where we define V_{O_i} as the set of all the triangular cells around the point O_i. In this case, we do not use the assumption that the computational domain Ω is convex. Unfortunately, it seems difficult to generalize this method to heterogeneous cases.

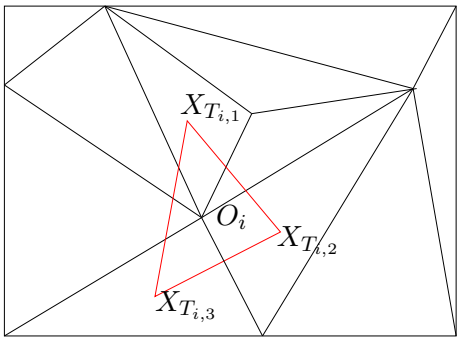

Figure 1: Grid composed of triangular cells

We use the same notations as that described in [EYM 99]. For $T \in \mathcal{T}$, we define (Figure 2):

- $S(T)$, the area of the triangular cell T, X_T the intersection of its angle bisectors, $c_j(T), j = 1, 2, 3$ the sides of T.
- $\vec{n}_{T,j}$ the outward directed normal vector to $c_j(T)$ to T with the same length as $c_j(T)$, for $j = 1, 2, 3$.

Let $\mathcal{A}_{ext}$ be the set of the edges belonging to $\partial\Omega$, $\mathcal{A}_{int}$, the set of interior edges. For $a \in \mathcal{A}_{int}$, we define:

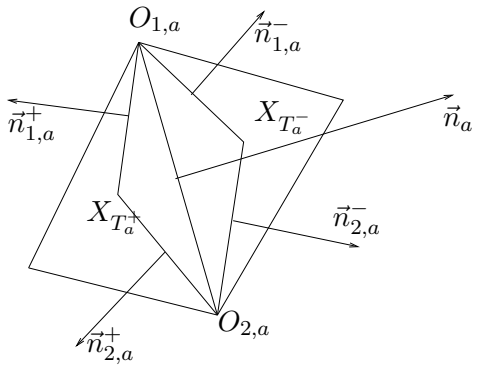

Figure 2: Homogeneous case

- T_a^+, T_a^- two triangular cells which share a common edge a, $O_{1,a}$, $O_{2,a}$ the two nodes of the edge a.
- $\vec{n}_a$, the normal vector to the segment $O_{1,a}O_{2,a}$ such as $\vec{n}_a$ is outward to T_a^+ with the same length as $O_{1,a}O_{2,a}$.
- $\vec{n}^+_{1,a}$, $\vec{n}^+_{2,a}$, $\vec{n}^-_{1,a}$ and $\vec{n}^-_{2,a}$ the normal vectors to the edges $X_{T_a^+}O_{1,a}$, $X_{T_a^+}O_{2,a}$, $X_{T_a^-}O_{1,a}$ and $X_{T_a^-}O_{2,a}$, respectively with the same length.
- $PT_{i,a}$ the triangular cell $(O_{i,a}, X_{T_a^+}, X_{T_a^-})$ with $SF_{i,a}$ its area and $\partial PT_{i,a}$ its boundary.

For $a \in \mathcal{A}_{ext}$, we also define:

- PT_a the triangular cell $(O_{1,a}, X_{T_a^+}, O_{2,a})$ with SF_a its area and ∂PT_a its boundary.

We use $SF_{i,a}\vec{q}_{i,a}$ to denote the value of $\int_{PT_{i,a}} \vec{q} d\Omega$ if $a \in \mathcal{A}_{int}$; we let $SF_a\vec{q}_a$ denote the value of $\int_{PT_a} \vec{q} d\Omega$ on PT_a if $a \in \mathcal{A}_{ext}$ and we let C_T denote the value of the concentration C at the point X_T. We approximate the value of the concentration C at the point $O_{i,a}$ with the expression $C_{O_{i,a}} = \sum_{\{1 \le j \le 3\}} \lambda_{i,j} C_{T_{i,j}}$.

Calculation of the flux $\vec{q} \cdot \vec{n_a}$

For an edge a belonging to $\mathcal{A}_{int}$, the integration of the first equation of system (1) on $PT_{i,a}$ using Green's formula leads to, for i=1,2:

$$\int_{PT_{i,a}} \vec{q} d\Omega = \int_{PT_{i,a}} \vec{\nabla} C d\Omega = \int_{\partial PT_{i,a}} C \vec{n} d\Gamma \tag{2}$$

Using a formula that is second order in space, we get, for $i = 1, 2$:

$$\vec{q}_{i,a} = \frac{1}{2SF_{i,a}} C_{O_{i,a}} (\vec{n}^+_{i,a} + \vec{n}^-_{i,a}) + \frac{1}{2SF_{i,a}} (-C_{T_a^-} \vec{n}^+_{i,a} - C_{T_a^+} \vec{n}^-_{i,a}) \tag{3}$$

We denote $\lambda_1 = \dfrac{(\vec{n}^+_{1,a} + \vec{n}^-_{1,a}) \cdot \vec{n_a}}{2SF_{1,a}}$, $\lambda_2 = \dfrac{(\vec{n}^+_{2,a} + \vec{n}^-_{2,a}) \cdot \vec{n_a}}{2SF_{2,a}}$, $\lambda_3 = -\dfrac{\vec{n}^+_{1,a} \cdot \vec{n_a}}{2SF_{1,a}}$ and $\lambda_4 = \dfrac{\vec{n}^-_{2,a} \cdot \vec{n_a}}{2SF_{2,a}}$.

The terms $\vec{q}_{1,a} \cdot \vec{n}_a$ and $\vec{q}_{2,a} \cdot \vec{n}_a$ can be written:

$$\vec{q}_{1,a} \cdot \vec{n}_a = \lambda_1 (C_{O_{1,a}} - C_{T_a^+}) + \lambda_3 (C_{T_a^-} - C_{T_a^+}) \tag{4}$$

and

$$\vec{q}_{2,a} \cdot \vec{n}_a = \lambda_2 (C_{O_{2,a}} - C_{T_a^-}) + \lambda_4 (C_{T_a^-} - C_{T_a^+}) \tag{5}$$

We remark that $\lambda_1 \lambda_2 \leq 0$. Let us assume: $\lambda_1 \geq 0$ and $\lambda_3 \leq \lambda_4$. If $C_{O_{1,a}} - C_{T_a^+} = 0$ (resp. $C_{O_{2,a}} - C_{T_a^-} = 0$), we choose $\vec{q} \cdot \vec{n_a} = \vec{q}_{1,a} \cdot \vec{n}_a$ (resp. $\vec{q} \cdot \vec{n_a} = \vec{q}_{2,a} \cdot \vec{n}_a$). Otherwise, using the same kind of combination described in [BER 06] and after discussion with [GAL 06], we define:

$$\vec{q} \cdot \vec{n}_a = \frac{|\lambda_2 (C_{O_{2,a}} - C_{T_a^-}) + (\lambda_4 - \lambda_3)(C_{T_a^-} - C_{T_a^+})| \vec{q}_{1,a} \cdot \vec{n}_a + |\lambda_1 (C_{O_{1,a}} - C_{T_a^+})| \vec{q}_{2,a} \cdot \vec{n}_a}{|\lambda_2 (C_{O_{2,a}} - C_{T_a^-}) + (\lambda_4 - \lambda_3)(C_{T_a^-} - C_{T_a^+})| + |\lambda_1 (C_{O_{1,a}} - C_{T_a^+})|} \tag{6}$$

In any case, $\vec{q} \cdot \vec{n}_a$ can be written: $\vec{q} \cdot \vec{n}_a = \mu_{1,a} \vec{q}_{1,a} \cdot \vec{n}_a + \mu_{2,a} \vec{q}_{2,a} \cdot \vec{n}_a$ with $\mu_{1,a} + \mu_{2,a} = 1$.

Remark 1: If $|\vec{q}_{1,a} \cdot \vec{n}_a| + |\vec{q}_{2,a} \cdot \vec{n}_a| \neq 0$, an other choice could be:

$$\vec{q} \cdot \vec{n}_a = \frac{|\vec{q}_{2,a} \cdot \vec{n}_a| \vec{q}_{1,a} \cdot \vec{n}_a + |\vec{q}_{1,a} \cdot \vec{n}_a| \vec{q}_{2,a} \cdot \vec{n}_a}{|\vec{q}_{2,a} \cdot \vec{n}_a| + |\vec{q}_{1,a} \cdot \vec{n}_a|} \tag{7}$$

Remark 2: any combination $(\mu_{1,a}, \mu_{2,a})$ with $\mu_{1,a} + \mu_{2,a} = 1$, and $\vec{q} \cdot \vec{n}_a = \mu_{1,a} \vec{q}_{1,a} \cdot \vec{n}_a + \mu_{2,a} \vec{q}_{2,a} \cdot \vec{n}_a$ gives a consistent formulation. For example, $\mu_{1,a} = 0.5$ and $\mu_{2,a} = 0.5$ leads to the so-called "diamond" scheme ([COU 99]).
Remark 3: if $\lambda_1 < 0$, the roles of $\vec{q}_{1,a} \cdot \vec{n}_a$ and $\vec{q}_{2,a} \cdot \vec{n}_a$ are reversed. If $\lambda_4 \leq \lambda_3$, we define:

$$\vec{q} \cdot \vec{n}_a = \frac{|\lambda_2 (C_{O_{2,a}} - C_{T_a^-})| \vec{q}_{1,a} \cdot \vec{n}_a + |\lambda_1 (C_{O_{1,a}} - C_{T_a^+}) + (\lambda_3 - \lambda_4)(C_{T_a^-} - C_{T_a^+})| \vec{q}_{2,a} \cdot \vec{n}_a}{|\lambda_2 (C_{O_{2,a}} - C_{T_a^-})| + |\lambda_1 (C_{O_{1,a}} - C_{T_a^+}) + (\lambda_3 - \lambda_4)(C_{T_a^-} - C_{T_a^+})|} \tag{8}$$

If the edge a belongs to $\mathcal{A}_{ext}$, we integrate the first equation of system (1) on the triangular cell PT_a and we impose the values of the boundary conditions at the points $O_{1,a}$ and $O_{2,a}$. We get:

$$\vec{q} \cdot \vec{n_a} = \vec{q_a} \cdot \vec{n_a} = \{ \frac{1}{2SF_a} C_{T_{a^+}} (\vec{n}_{1,a}^+ + \vec{n}_{2,a}^+) + \frac{1}{2SF_a} (-C_{O_{1,a}} \vec{n}_{2,a}^+ - C_{O_{2,a}} \vec{n}_{1,a}^+) \} \cdot \vec{n_a} \tag{9}$$

Calculation of the main unknown C_T
Let us integrate the mass conservation equation (the second equation of system (1)) over T. We get:

$$\int_T \omega \frac{\partial C}{\partial t} d\Omega = S(T) \omega \frac{\partial C_T}{\partial t} = \int_T div \vec{q} d\Omega = \int_{\partial T} \vec{q}.\vec{n} d\Gamma = \sum_{j=1}^{j=3} \vec{q}.\vec{n}_{T,j} \tag{10}$$

2.2 Properties of the algorithm

First, we use the following definition:
a matrix A is a strictly diagonally dominant M-Matrix if and only if its coefficients a_{ij} *satisfy :*

$$\begin{cases} a_{ii} > 0 \\ a_{ij} \leq 0 \\ a_{kk} > \sum_{j \neq k} |a_{kj}| \ \forall k \end{cases} \tag{11}$$

We let SF denote the diagonal matrix with coefficients equal to the areas of the grid, Δt the time step, $C^n = C(n\Delta t)$ the vector of the main unknowns and $A(C^n)$ the discretization matrix of $div\overline{\overline{D}}\vec{\nabla}$ of dimension N_{ma}. We choose an implicit time scheme. The discretization of the equation (10) leads to:
$(SF\omega - \Delta t A(C^{n+1}))C^{n+1} = SF\omega C^n$ and we denote $M = SF\omega - \Delta t A(C^{n+1})$.
Proposition 2. *For any triangular cell, the matrix M is a strictly diagonally dominant M-matrix.*
Proof
If the edge $a \in \mathcal{A}_{int}$, and
$\left\{\lambda_1(C_{O_{1,a}} - C_{T_a^+})\right\}\left\{\lambda_2(C_{O_{2,a}} - C_{T_a^-}) + (\lambda_4 - \lambda_3)(C_{T_a^-} - C_{T_a^+})\right\} > 0$, equality (6) becomes:

$$\begin{cases} \vec{q}\cdot\vec{n}_a = \dfrac{2\lambda_1(C_{O_{1,a}} - C_{T_a^+})|\lambda_2(C_{O_{2,a}} - C_{T_a^-}) + (\lambda_4 - \lambda_3)(C_{T_a^-} - C_{T_a^+})|}{|\lambda_2(C_{O_{2,a}} - C_{T_a^-}) + (\lambda_4 - \lambda_3)(C_{T_a^-} - C_{T_a^+})| + |\lambda_1(C_{O_{1,a}} - C_{T_a^+})|} \\ \qquad +\lambda_3(C_{T_a^-} - C_{T_a^+}) = \\ \dfrac{2|\lambda_1(C_{O_{1,a}} - C_{T_a^+})|\left\{\lambda_2(C_{O_{2,a}} - C_{T_a^-}) + (\lambda_4 - \lambda_3)(C_{T_a^-} - C_{T_a^+})\right\}}{|\lambda_2(C_{O_{2,a}} - C_{T_a^-}) + (\lambda_4 - \lambda_3)(C_{T_a^-} - C_{T_a^+})| + |\lambda_1(C_{O_{1,a}} - C_{T_a^+})|} \\ \qquad +\lambda_3(C_{T_a^-} - C_{T_a^+}) \end{cases} \tag{12}$$

If the edge $a \in \mathcal{A}_{int}$, and
$\left\{\lambda_1(C_{O_{1,a}} - C_{T_a^+})\right\}\left\{\lambda_2(C_{O_{2,a}} - C_{T_a^-}) + (\lambda_4 - \lambda_3)(C_{T_a^-} - C_{T_a^+})\right\} \leq 0$, the flux $\vec{q}.\vec{n}_a$ can be written :

$$\vec{q}\cdot\vec{n}_a = \lambda_3(C_{T_a^-} - C_{T_a^+})$$

In any case, we deduce that the flux $\vec{q}\cdot\vec{n}_a$ can be written:

$$\vec{q}\cdot\vec{n}_a = f_1(C_{O_{1,a}}, C_{O_{2,a}}, C_{T_a^-}, C_{T_a^+})(C_{T_a^-} - C_{T_a^+}) + g_1(C_{O_{1,a}}, C_{O_{2,a}}, C_{T_a^-}, C_{T_a^+})(C_{O_{1,a}} - C_{T_a^+})$$

with f_1 and g_1 two positive functions. This is the flux coming from the cell T_a^+. Moreover, the flux $\vec{q}\cdot(-\vec{n}_a)$ can be written:

$$\vec{q}\cdot(-\vec{n}_a) = f_2(C_{O_{1,a}}, C_{O_{2,a}}, C_{T_a^-}, C_{T_a^+})(C_{T_a^+} - C_{T_a^-}) + g_2(C_{O_{1,a}}, C_{O_{2,a}}, C_{T_a^-}, C_{T_a^+})(C_{O_{2,a}} - C_{T_a^-})$$

with f_2 and g_2 two positive functions. This is the flux coming from the cell T_a^-.
If $a \in \mathcal{A}_{ext}$, $\vec{q}\cdot\vec{n}_a$ can be rewritten:

$$\vec{q}\cdot\vec{n}_a = f_3(C_{O_{1,a}} - C_{T_a^+}) + f_4(C_{O_{2,a}} - C_{T_a^+})$$

with $f_3 = \dfrac{-\vec{n}_{2,a}^+\cdot\vec{n_a}}{2SF_a}$ and $f_4 = \dfrac{-\vec{n}_{1,a}^+\cdot\vec{n_a}}{2SF_a}$ which are also positive functions.
Let $V(T_a^+)$ be the stencil used to calculate $\vec{q}\cdot\vec{n}_a$ and let $V(T_a^-)$ be the stencil used to calculate $\vec{q}\cdot(-\vec{n}_a)$.
In any case, we get $\vec{q}\cdot\vec{n}_a = \sum_{j\in V(T_a^+)} f_{5,j}(C_j - C_{T_a^+})$ and
$\vec{q}\cdot(-\vec{n}_a) = \sum_{j\in V(T_a^-)} f_{6,j}(C_j - C_{T_a^-})$, where $f_{5,j}$ and $f_{6,j}$ are deduced from the functions f_1 through f_4. We conclude the off-diagonal entries of the matrix M are negative. Moreover, for all cells, the diagonal term is strictly greater than the sum of off-diagonal entries because the coefficients of the diagonal matrix SF are strictly positive. We conclude that the matrix M is a strictly diagonally dominant M-Matrix. ■

Remark 1 *The flux approximation is consistent because we only use a second order in space formula.*

Remark 2 *Using properties of strictly diagonally dominant M-matrices, the previous scheme, denoted VFPMMD, satisfies discrete maximum and minimum principles. Moreover, the calculated solution has no local extrema.*

2.3 Anisotropic heterogeneous case

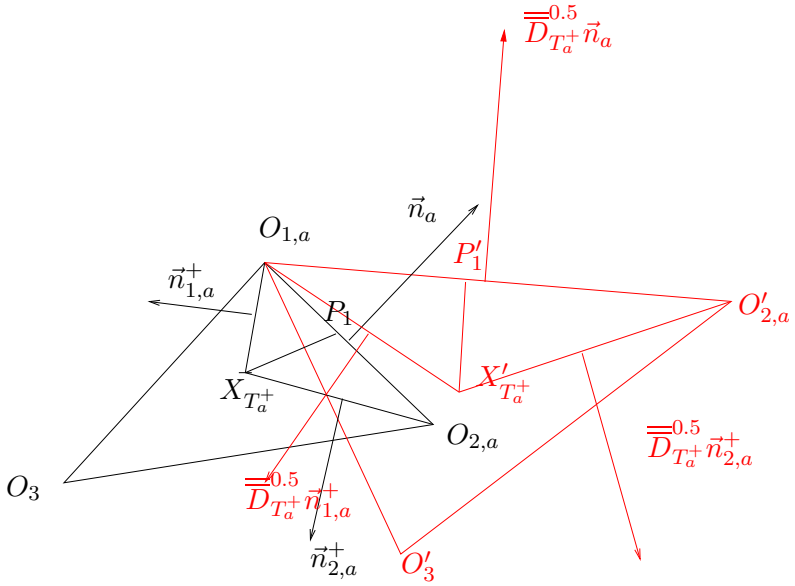

Figure 3: Image of a triangular cell by the application $R(-\frac{\pi}{2})\overline{\overline{D}}^{0.5}_{T_a^+}R(\frac{\pi}{2})$

We let $\overline{\overline{D}}_{T_a^+}$ denote the value of $\dfrac{\int_{T_a^+}\overline{\overline{D}}d\Omega}{\int_{T_a^+}d\Omega}$ and $R(\theta)$ the rotation of angle θ.

Proposition 3. *There exists one point $X_{T_a^+}$ inside each triangular cell $T_a^+ \in \mathcal{T}$ and*

a point P_1 (respectively P_2 and P_3) between the two nodes of $O_{1,a}, O_{2,a}$ (respectively $O_{2,a}, O_3$ and $O_3, O_{1,a}$) such that : $R(\frac{\pi}{2})\vec{O_{1,a}P_1}.\overline{\overline{D}}_{T_a^+}R(\frac{\pi}{2})\vec{X_{T_a^+}P_1} = 0$ (respectively $R(\frac{\pi}{2})\vec{O_{2,a}P_2}.\overline{\overline{D}}_{T_a^+}R(\frac{\pi}{2})\vec{X_{T_a^+}P_2} = 0$ and $R(\frac{\pi}{2})\vec{O_3P_3}.\overline{\overline{D}}_{T_a^+}R(\frac{\pi}{2})\vec{X_{T_a^+}P_3} = 0$)

Proof

We consider a triangular cell T_a^+ with vertices $O_{1,a}, O_{2,a}, O_3$. Since the tensor $\overline{\overline{D}}_{T_a^+}$ is symmetric positive definite, we denote $\overline{\overline{D}}^{0.5}_{T_a^+}$, such that $D_{T_a^+} = \left\{\overline{\overline{D}}^{0.5}_{T_a^+}\right\}^2$, with positive eigenvalues. Let $R(-\frac{\pi}{2})\overline{\overline{D}}^{0.5}_{T_a^+}R(\frac{\pi}{2})T_a^+$ be the image of T_a^+ with vertices $O_{1,a}O'_{2,a}O'_3$ which satisfies (Figure 3):

$\vec{O_{1,a}O'_{2,a}} = R(-\frac{\pi}{2})\overline{\overline{D}}^{0.5}_{T_a^+}R(\frac{\pi}{2})\vec{O_{1,a}O_{2,a}}$ and $\vec{O_{1,a}O'_3} = R(-\frac{\pi}{2})\overline{\overline{D}}^{0.5}_{T_a^+}R(\frac{\pi}{2})\vec{O_{1,a}O_3}$.

The point $X'_{T_a^+}$, which is the center of the circle inscribed in the triangular cell $O_{1,a}O'_{2,a}O'_3$, satisfies the following equality:

$$\vec{O_{1,a}X'_{T_a^+}} = \frac{\vec{O_{1,a}O'_{2,a}}|O_{1,a}O'_3| + \vec{O_{1,a}O'_3}|O_{1,a}O'_{2,a}|}{|O'_{2,a}O'_3| + |O_{1,a}O'_3| + |O_{1,a}O'_{2,a}|} .$$

We define the point $X_{T_a^+}$ as the inverse image of the point $X'_{T_a^+}$.

It satisfies the equality:

$$\vec{O_{1,a}X_{T_a^+}} = R(\frac{\pi}{2})\overline{\overline{D}}^{-0.5}_{T_a^+}R(-\frac{\pi}{2})\vec{O_{1,a}X'_{T_a^+}} .$$

This can also be written:

$$\vec{O_{1,a}X_{T_a^+}} = \frac{\vec{O_{1,a}O_{2,a}}|O_{1,a}O'_3| + \vec{O_{1,a}O_3}|O_{1,a}O'_{2,a}|}{|O'_{2,a}O'_3| + |O_{1,a}O'_3| + |O_{1,a}O'_{2,a}|} .$$

Since the values $\frac{|O_{1,a}O'_3|}{|O'_{2,a}O'_3|+|O_{1,a}O'_3|+|O_{1,a}O'_{2,a}}$ and $\frac{|O_{1,a}O'_{2,a}|}{|O'_{2,a}O'_3|+|O_{1,a}O'_3|+|O_{1,a}O'_{2,a}}$ are positive, the point $X_{T_a^+}$ is inside the triangular cell T_a^+.

Moreover, there exists a point P'_1 between the two nodes of $O_{1,a}O'_{2,a}$ such that $\vec{O_{1,a}P'_1}.\vec{X'_{T_a^+}P'_1} = 0$, using properties on intersections of angle bisectors of a triangular cell. Let be P_1 the inverse image of the point P'_1. Using properties of linear applications, the point P_1 is between the two nodes of $O_{1,a}O_{2,a}$. Then, we obtain the equalities:

$R(-\frac{\pi}{2})\overline{\overline{D}}^{0.5}_{T_a^+}R(\frac{\pi}{2})\vec{O_{1,a}P_1}.R(-\frac{\pi}{2})\overline{\overline{D}}^{0.5}_{T_a^+}R(\frac{\pi}{2})\vec{X_{T_a^+}P_1} = 0.$

Using matrix notations, we get :

${}^t\{R_m(-\frac{\pi}{2})\overline{\overline{D}}^{0.5}_{m,T_a^+}R_m(\frac{\pi}{2})O_{1,a}P_1\}R_m(-\frac{\pi}{2})\overline{\overline{D}}^{0.5}_{m,T_a^+}R_m(\frac{\pi}{2})X_{T_a^+}P_1 = 0$

where we denote ^{t} the conjugate, $O_{1,a}P_1$, $X_{T_a^+}P_1$ the components of $\vec{O_{1,a}P_1}$, $\vec{X_{T_a^+}P_1}$, R_m the matrix associated with the application R, and $\overline{\overline{D}}^{0.5}_{m,T_a^+}$ the matrix associated with the application $\overline{\overline{D}}^{0.5}_{T_a^+}$.

Then, we obtain :

${}^t(R_m(\frac{\pi}{2})O_{1,a}P_1)\overline{\overline{D}}^{0.5}_{m,T_a^+}{}^tR_m(-\frac{\pi}{2})R_m(-\frac{\pi}{2})\overline{\overline{D}}^{0.5}_{m,T_a^+}R_m(\frac{\pi}{2})X_{T_a^+}P_1 = 0$

The equality becomes :

${}^t(R_m(\frac{\pi}{2})O_{1,a}P_1)\overline{\overline{D}}_{m,T_a^+}R_m(\frac{\pi}{2})X_{T_a^+}P_1 = 0.$
We finally obtain :
$R(\frac{\pi}{2})\vec{O_{1,a}P_1}.\overline{\overline{D}}_{T_a^+}R(\frac{\pi}{2})\vec{X_{T_a^+}P_1} = 0$. Using the same kind of calculations, we show there exists two points P_2 en P_3 satisfying : $R(\frac{\pi}{2})\vec{O_{2,a}P_2}.\overline{\overline{D}}_{T_a^+}R(\frac{\pi}{2})\vec{X_{T_a^+}P_2} = 0$ and $R(\frac{\pi}{2})\vec{O_3P_3}.\overline{\overline{D}}_{T_a^+}R(\frac{\pi}{2})\vec{X_{T_a^+}P_3} = 0$. ■

Finally, let us note that we also obtain the inequalities :
$R(\frac{\pi}{2})O_{1,a}\vec{X'}_{T_a^+}.R(\frac{\pi}{2})O_{1,a}\vec{O'}_{2,a} \geq 0$
Using matrix notations, we get :
${}^t\{\overline{\overline{D}}^{0.5}_{m,T_a^+}R_m(\frac{\pi}{2})O_{1,a}X_{T_a^+}\}\overline{\overline{D}}^{0.5}_{m,T_a^+}R_m(\frac{\pi}{2})O_{1,a}O_{2,a} \geq 0.$
This inequality becomes :
${}^t(R_m(\frac{\pi}{2})O_{1,a}X_{T_a^+})\overline{\overline{D}}^{0.5}_{m,T_a^+}\overline{\overline{D}}^{0.5}_{m,T_a^+}R_m(\frac{\pi}{2})O_{1,a}O_{2,a} \geq 0$, which can be rewritten :
$R(\frac{\pi}{2})O_{1,a}\vec{X}_{T_a^+}.\overline{\overline{D}}_{T_a^+}R(\frac{\pi}{2})O_{1,a}\vec{O}_{2,a} \geq 0.$
which can be rewritten: $\vec{n}^+_{1,a} \cdot \overline{\overline{D}}_{T_a^+}\vec{n}_a \leq 0$
Using the same kind of calculations, we also get : $\vec{n}^+_{2,a} \cdot \overline{\overline{D}}_{T_a^+}\vec{n}_a \leq 0$.

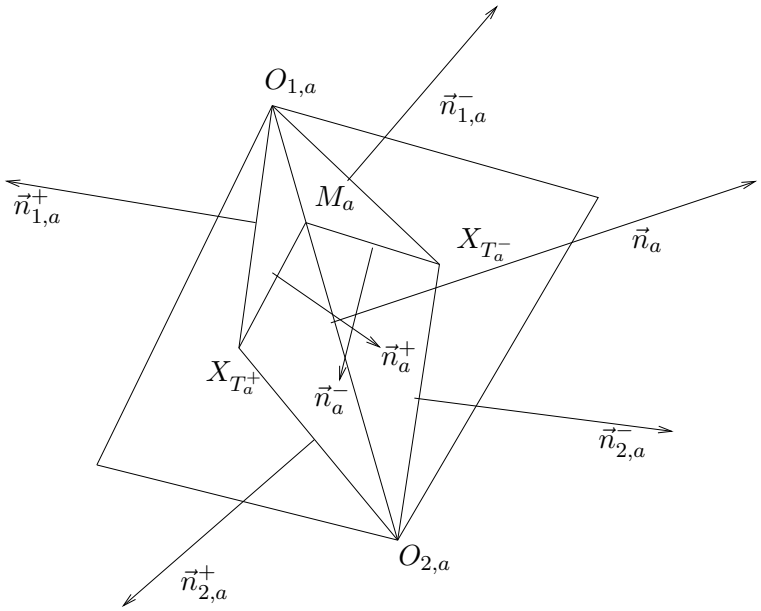

Figure 4: Heterogeneous case

The set $\mathcal{B}$ is now defined as the set of points X_T defined in proposition 3 and with the points located at the midpoints of the edges of the boundary.
Calculation of the gradients
We introduce the additional following notations:

- the point M_a is the point on the edge $O_{1,a}, O_{2,a}$ defined in proposition 3.

- $SF_{i,a}^{+}$ (resp. $SF_{i,a}^{-}$) the area of the triangular cell $O_{i,a}X_{T_a^+}M_a$ (resp. $O_{i,a}X_{T_a^-}M_a$).
- $C_{i,a}$ the value of the concentration at the point M_a associated with $O_{i,a}$, $SF_{i,a}^{+}q_{i,a}^{+}$ (resp. $SF_{i,a}^{-}q_{i,a}^{-}$) the value of the vector $\int_{O_{i,a}X_{T_a^+}M_a}\vec{q}d\Omega$ (resp. $\int_{O_{i,a}X_{T_a^-}M_a}\vec{q}d\Omega$).

Using a formula that is second order in space, equation (3) becomes for $i=1$:

$$\begin{cases} \overline{\overline{D}}_{T_a^+}^{-1}\vec{q}_{1,a}^{+} = \dfrac{1}{2SF_{1,a}^{+}}(C_{T_a^+}-C_{1,a})\vec{n}_{1,a}^{+} + \dfrac{1}{2SF_{1,a}^{+}}(C_{T_a^+}-C_{O_{1,a}})\vec{n}_a^{+} \\ \overline{\overline{D}}_{T_a^-}^{-1}\vec{q}_{1,a}^{-} = \dfrac{1}{2SF_{1,a}^{-}}(C_{T_a^-}-C_{1,a})\vec{n}_{1,a}^{-} + \dfrac{1}{2SF_{1,a}^{-}}(C_{T_a^-}-C_{O_{1,a}})\vec{n}_a^{-} \end{cases} \tag{13}$$

and for $i=2$:

$$\begin{cases} \overline{\overline{D}}_{T_a^+}^{-1}\vec{q}_{2,a}^{+} = \dfrac{1}{2SF_{2,a}^{+}}(C_{T_a^+}-C_{2,a})\vec{n}_{2,a}^{+} - \dfrac{1}{2SF_{2,a}^{+}}(C_{T_a^+}-C_{O_{2,a}})\vec{n}_a^{+} \\ \overline{\overline{D}}_{T_a^-}^{-1}\vec{q}_{2,a}^{-} = \dfrac{1}{2SF_{2,a}^{-}}(C_{T_a^-}-C_{2,a})\vec{n}_{2,a}^{-} - \dfrac{1}{2SF_{2,a}^{-}}(C_{T_a^-}-C_{O_{2,a}})\vec{n}_a^{-} \end{cases} \tag{14}$$

Calculation of $C_{i,a}$

We delete the additional unknowns $C_{i,a}$ by imposing flux continuity, that is to say, $\vec{q}_{i,a}^{+}\cdot\vec{n}_a = \vec{q}_{i,a}^{-}\cdot\vec{n}_a$. Since $\vec{n}_a\cdot\overline{\overline{D}}_{T_a^+}\vec{n}_a^{+}=0$ using the definition of M_a, the concentration $C_{1,a}$ satisfies:

$$\begin{cases} (\dfrac{1}{SF_{1,a}^{-}}\vec{n}_a\cdot\overline{\overline{D}}_{T_a^-}\vec{n}_{1,a}^{-} - \dfrac{1}{SF_{1,a}^{+}}\vec{n}_a\cdot\overline{\overline{D}}_{T_a^+}\vec{n}_{1,a}^{+})C_{1,a} = \\ -\dfrac{1}{SF_{1,a}^{+}}\vec{n}_a\cdot\overline{\overline{D}}_{T_a^+}\vec{n}_{1,a}^{+}C_{T_a^+} + \dfrac{1}{SF_{1,a}^{-}}\vec{n}_a\cdot\overline{\overline{D}}_{T_a^-}\vec{n}_{1,a}^{-}C_{T_a^-} + \dfrac{1}{SF_{1,a}^{-}}\vec{n}_a\cdot\overline{\overline{D}}_{T_a^-}\vec{n}_a^{-}(C_{T_a^-}-C_{O_{1,a}}) \end{cases} \tag{15}$$

Moreover, the concentration $C_{2,a}$ satisfies:

$$\begin{cases} (\dfrac{1}{SF_{2,a}^{-}}\vec{n}_a\cdot\overline{\overline{D}}_{T_a^-}\vec{n}_{2,a}^{-} - \dfrac{1}{SF_{2,a}^{+}}\vec{n}_a\cdot\overline{\overline{D}}_{T_a^+}\vec{n}_{2,a}^{+})C_{2,a} = \\ -\dfrac{1}{SF_{2,a}^{+}}\vec{n}_a\cdot\overline{\overline{D}}_{T_a^+}\vec{n}_{2,a}^{+}C_{T_a^+} + \dfrac{1}{SF_{2,a}^{-}}\vec{n}_a\cdot\overline{\overline{D}}_{T_a^-}\vec{n}_{2,a}^{-}C_{T_a^-} - \dfrac{1}{SF_{2,a}^{-}}\vec{n}_a\cdot\overline{\overline{D}}_{T_a^-}\vec{n}_a^{-}(C_{T_a^-}-C_{O_{2,a}}) \end{cases} \tag{16}$$

Using properties on $\mathcal{B}$, we get the following inequalities: $\vec{n}_a\cdot\overline{\overline{D}}_{T_a^+}\vec{n}_{i,a}^{+}\leq 0$ and $\vec{n}_a\cdot\overline{\overline{D}}_{T_a^-}\vec{n}_{i,a}^{-}\geq 0$. We conclude that $C_{1,a}$ and $C_{2,a}$ can be simplified in the following way:

$$C_{1,a} = \alpha_1 C_{T_a^+} + \beta_1 C_{T_a^-} + \gamma_1 C_{O_{1,a}}$$

and

$$C_{2,a} = \alpha_2 C_{T_a^+} + \beta_2 C_{T_a^-} + \gamma_2 C_{O_{2,a}}$$

with α_1, α_2, β_1, β_2 positive coefficients, $\gamma_1\gamma_2 \leq 0$, $\alpha_1+\beta_1+\gamma_1=1$ and $\alpha_2+\beta_2+\gamma_2=1$.

Calculation of the flux $\vec{q}\cdot\vec{n}_a$

We conclude that the flux $\vec{q}_{1,a}\cdot\vec{n}_a$ and $\vec{q}_{2,a}\cdot\vec{n}_a$ can be written in the following way:

$$\vec{q}_{1,a}\cdot\vec{n}_a = -\frac{1}{SF^+_{1,a}}\vec{n}_a\cdot\overline{\overline{D}}_{T_a^+}\vec{n}^+_{1,a}\left\{\beta_1(C_{T_a^-}-C_{T_a^+})+\gamma_1(C_{O_{1,a}}-C_{T_a^+})\right\}$$

and

$$\vec{q}_{2,a}\cdot\vec{n}_a = -\frac{1}{SF^+_{2,a}}\vec{n}_a\cdot\overline{\overline{D}}_{T_a^+}\vec{n}^+_{2,a}\left\{\beta_2(C_{T_a^-}-C_{T_a^+})+\gamma_2(C_{O_{2,a}}-C_{T_a^-})\right\}\ .$$

We rewrite these equalities as

$$\vec{q}_{1,a}\cdot\vec{n}_a = \lambda'_1(C_{O_{1,a}}-C_{T_a^+})+\lambda'_3(C_{T_a^-}-C_{T_a^+})$$

and

$$\vec{q}_{2,a}\cdot\vec{n}_a = \lambda'_2(C_{O_{2,a}}-C_{T_a^-})+\lambda'_4(C_{T_a^-}-C_{T_a^+})\ .$$

with $\lambda'_1 = -\frac{1}{SF^+_{1,a}}\vec{n}_a\cdot\overline{\overline{D}}_{T_a^+}\vec{n}^+_{1,a}\gamma_1$, $\lambda'_2 = -\frac{1}{SF^+_{2,a}}\vec{n}_a\cdot\overline{\overline{D}}_{T_a^+}\vec{n}^+_{2,a}\gamma_2$,
$\lambda'_3 = -\frac{1}{SF^+_{1,a}}\vec{n}_a\cdot\overline{\overline{D}}_{T_a^+}\vec{n}^+_{1,a}\beta_1$ and $\lambda'_4 = -\frac{1}{SF^+_{2,a}}\vec{n}_a\cdot\overline{\overline{D}}_{T_a^+}\vec{n}^+_{2,a}\beta_2$.

Let us assume that $\lambda'_1\geq 0$ (if $\lambda'_1\leq 0$, the roles of $\vec{q}_{1,a}\cdot\vec{n}_a$ and $\vec{q}_{2,a}\cdot\vec{n}_a$ are reversed). We recognize the same kind of equalities described in the homogeneous case for equations (4) and (5). The important point is that λ'_3 and λ'_4 are positive coefficients and that $\lambda'_1\lambda'_2\leq 0$. For example, if $\lambda'_3\leq\lambda'_4$, we can choose for $a\in\mathcal{A}_{int}$, $\vec{q}\cdot\vec{n}_a$ in the form:

$$\vec{q}\cdot\vec{n}_a = \frac{|\lambda'_2(C_{O_{2,a}}-C_{T_a^-})+(\lambda'_4-\lambda'_3)(C_{T_a^-}-C_{T_a^+})|\vec{q}_{1,a}\cdot\vec{n}_a+|\lambda'_1(C_{O_{1,a}}-C_{T_a^+})|\vec{q}_{2,a}\cdot\vec{n}_a}{|\lambda'_2(C_{O_{2,a}}-C_{T_a^-})+(\lambda'_4-\lambda'_3)(C_{T_a^-}-C_{T_a^+})|+|\lambda'_1(C_{O_{1,a}}-C_{T_a^+})|} \tag{17}$$

As the flux can be written in the same way as in the homogeneous case, the resulting global matrix is also a strictly diagonally dominant M-matrix. We conclude that the scheme satisfies minimum and maximum principles without conditions on the tensor.

2.4 Discrete system

2.4.1 Implicit scheme

We solve the equation (10) : $(SF\omega-\Delta tA(C^{n+1}))C^{n+1}=SF\omega C^n$. We use a fixed point algorithm to treat the non linearity. We get:

$$(SF\omega-\Delta tA(C^i))C^{i+1}=SF\omega C^i$$

where i is a fixed point iteration.

Method 1
We choose to calculate the following fluxes:

$$\vec{q}^{i+1}.\vec{n}_a = \frac{|\lambda_2(C^i_{O_{2,a}} - C^i_{T_a^-}) + (\lambda_4 - \lambda_3)(C^i_{T_a^-} - C^i_{T_a^+})|\vec{q}^{i+1}_{1,a} \cdot \vec{n}_a + |\lambda_1(C^i_{O_{1,a}} - C^i_{T_a^+})|\vec{q}^{i+1}_{2,a} \cdot \vec{n}_a}{|\lambda_2(C^i_{O_{2,a}} - C^i_{T_a^-}) + (\lambda_4 - \lambda_3)(C^i_{T_a^-} - C^i_{T_a^+})| + |\lambda_1(C^i_{O_{1,a}} - C^i_{T_a^+})|} \tag{18}$$

For any iteration of the chosen algorithm, these fluxes are consistent because they can be written in the following way:

$$\vec{q}^{i+1} \cdot \vec{n}_a = (\theta^i_a \vec{q}^{i+1}_{1,a} \cdot \vec{n}_a) + ((1. - \theta^i_a)\vec{q}^{i+1}_{2,a} \cdot \vec{n}_a)$$

Moreover, for any iteration, the scheme is locally conservative. However, minimum and maximum principles are satisfied once the convergence criterion is achieved. In some cases, one iteration in the fixed point algorithm can be sufficient to obtain the desired properties.
Note: this is the method we use in the numerical results.

Method 2
Another technique consists of inverting a strictly diagonally dominant M-Matrix at any iteration and the local conservation and the consistence of the scheme is obtained once the convergence of the algorithm is achieved. For any iteration, minimum and maximum principles are satisfied. We calculate two fluxes at each face which can be written:

$$\begin{cases} \vec{q}_{1,a} \cdot \vec{n}_a = \lambda_3(C^{i+1}_{T_a^-} - C^{i+1}_{T_a^+}) + 2\lambda_1 coef_1(C^{i+1}_{O_{1,a}} - C^{i+1}_{T_a^+}) \\ \quad if \ \left\{\lambda_1(C^i_{O_{1,a}} - C^i_{T_a^+})\right\}\left\{\lambda_2(C^i_{O_{2,a}} - C^i_{T_a^-}) + (\lambda_4 - \lambda_3)(C^i_{T_a^-} - C^i_{T_a^+})\right\} > 0 \\ \vec{q}_{1,a} \cdot \vec{n}_a = \lambda_3(C^{i+1}_{T_a^-} - C^{i+1}_{T_a^+}) \\ \quad if \ \left\{\lambda_1(C^i_{O_{1,a}} - C^i_{T_a^+})\right\}\left\{\lambda_2(C^i_{O_{2,a}} - C^i_{T_a^-}) + (\lambda_4 - \lambda_3)(C^i_{T_a^-} - C^i_{T_a^+})\right\} \leq 0 \end{cases} \tag{19}$$

$$\begin{cases} \vec{q}_{2,a} \cdot \vec{n}_a = \lambda_3(C^{i+1}_{T_a^-} - C^{i+1}_{T_a^+}) + 2coef_2\left\{\lambda_2(C^{i+1}_{O_{2,a}} - C^{i+1}_{T_a^-}) + (\lambda_4 - \lambda_3)(C^{i+1}_{T_a^-} - C^{i+1}_{T_a^+})\right\} \\ \quad if \ \left\{\lambda_1(C^i_{O_{1,a}} - C^i_{T_a^+})\right\}\left\{\lambda_2(C^i_{O_{2,a}} - C^i_{T_a^-}) + (\lambda_4 - \lambda_3)(C^i_{T_a^-} - C^i_{T_a^+})\right\} > 0 \\ \vec{q}_{2,a} \cdot \vec{n}_a = \lambda_3(C^{i+1}_{T_a^-} - C^{i+1}_{T_a^+}) \\ \quad if \ \left\{\lambda_1(C^i_{O_{1,a}} - C^i_{T_a^+})\right\}\left\{\lambda_2(C^i_{O_{2,a}} - C^i_{T_a^-}) + (\lambda_4 - \lambda_3)(C^i_{T_a^-} - C^i_{T_a^+})\right\} \leq 0 \end{cases} \tag{20}$$

where

$$coef_1 = \frac{|\lambda_2(C^i_{O_{2,a}} - C^i_{T_a^-}) + (\lambda_4 - \lambda_3)(C^i_{T_a^-} - C^i_{T_a^+})|}{|\lambda_2(C^i_{O_{2,a}} - C^i_{T_a^-}) + (\lambda_4 - \lambda_3)(C^i_{T_a^-} - C^i_{T_a^+})| + |\lambda_1(C^i_{O_{1,a}} - C^i_{T_a^+})|}$$

and

$$coef_2 = \frac{|\lambda_1(C^i_{O_{1,a}} - C^i_{T_a^+})|}{|\lambda_2(C^i_{O_{2,a}} - C^i_{T_a^-}) + (\lambda_4 - \lambda_3)(C^i_{T_a^-} - C^i_{T_a^+})| + |\lambda_1(C^i_{O_{1,a}} - C^i_{T_a^+})|}$$

2.4.2 Semi-implicit scheme

We solve the following equation:

$$(SF\omega - \Delta t A(C^n))C^{n+1} = SF\omega C^n$$

This scheme corresponds to one iteration in the fixed point algorithm described previously. If we use the method 2, we obtain minimum and the maximum principles but the scheme is convergent if the time step Δt is small enough.

2.5 Generalization to 3 dimensions

The scheme presented in [LP 05b] have been developed in [KAP 07] in 3 dimensions. Using the same kind of method, it should be easy to generalize the VFPMMD scheme with tetrahedrons.

3 Numerical results

3.1 Stationary case

In order to evaluate the accuracy of the scheme, let us consider the following elliptic problem:

$$\left\{ \begin{array}{l} div(\overline{\overline{D}}\vec{\nabla}C) = -S \text{ on } \Omega =]0, 0.5[\times]0, 0.5[\\ C = sin(\pi x)sin(\pi y) \ for \ (x, y) \in \partial\Omega \end{array} \right. \text{with } \overline{\overline{\mathrm{D}}} = \left(\begin{array}{cc} y_1^2 + \epsilon x_1^2 & -(1-\epsilon)x_1 y_1 \\ -(1-\epsilon)x_1 y_1 & x_1^2 + \epsilon y_1^2 \end{array} \right) \tag{21}$$

and

$$\left\{ \begin{array}{c} S = sin(\pi x)sin(\pi y)((1+\epsilon)\pi^2(x_1^2 + y_1^2)) + cos(\pi x)sin(\pi y)((1-3\epsilon)\pi x_1) \\ +sin(\pi x)cos(\pi y)((1-3\epsilon)\pi y_1) + cos(\pi x)cos(\pi y)(2\pi^2(1-\epsilon)x_1 y_1) \end{array} \right. \tag{22}$$

where $x_1 = x + 10^{-3}$ and $y_1 = y + 10^{-3}$. The parameter ϵ is equal to 10^{-3}. Calculating the eigenvalues $(y_1^2 + x_1^2)$ and $\epsilon(y_1^2 + x_1^2)$, it is clear that the anisotropy ratio is equal to 10^3. The analytical solution can be written: $C = sin(\pi x)sin(\pi y)$. We consider five grids, made up of about 30 cells (the first) to 38000 cells (the fifth). To treat the non-linearity, we perform a few iterations of a fixed point algorithm. The convergence criterion is achieved when the relative difference in L^2 norm between two iterations is less than 10^{-5}. Since S is negative, the scheme satisfies the minimum principle if and only if the computed solution is positive and if no local minima appear. We show in Table 2 the L^2 errors for C with respect to the analytical solution, the number of iterations (nit) in the fixed point algorithm, and the percentage of local minima (nlm) as a function of the discretization step h for unstructured triangular cells. We notice that the order in space of the method tends toward 2. We check that the solution has no local minima. We note a small loss of precision with respect to the VFMON scheme ([LP 05b]) which is of order 2 in space on this computation (Table 1). Let us recall, that this scheme satisfies the minimum or the maximum principle but not the both simultaneously. Moreover, we also show the results obtained with

a non-monotone linear scheme, the so-called "diamond" scheme ([COU 99]) (Table 3). We calculate the flux $\vec{q}\cdot\vec{n}_a$ in the following way:

$$\vec{q}\cdot\vec{n}_a = (0.5\vec{q}_{1,a}\cdot\vec{n}_a) + (0.5\vec{q}_{2,a}\cdot\vec{n}_a)$$

We notice the scheme is of order 2 in space. It is more accurate than the VFMON scheme. However, we observe a few oscillations with amplitudes ranging from 10^{-3} (third grid) to 10^{-5} for the fifth grid. Finally, we performed the results obtained with one iteration in the fixed point algorithm (Table 4). Even though the fixed point algorithm has not converged, we notice that the solution has no local minima. So, sometimes, it is sufficient to perform only a few iterations to obtain the desired properties.

h	$\frac{1}{8}$	$\frac{1}{16}$	$\frac{1}{32}$	$\frac{1}{64}$	$\frac{1}{128}$	$\frac{1}{256}$
L^2 error	4.2×10^{-2}	1.0×10^{-2}	2.7×10^{-3}	7.2×10^{-4}	1.6×10^{-4}	4.0×10^{-5}

Table 1: L^2 error as a function of the discretization step for the VFMON scheme

h	$\frac{1}{8}$	$\frac{1}{16}$	$\frac{1}{32}$	$\frac{1}{64}$	$\frac{1}{128}$	$\frac{1}{256}$
L^2 error	4.6×10^{-2}	1.4×10^{-2}	4.14×10^{-3}	1.13×10^{-3}	4×10^{-4}	1×10^{-4}
nit	15	45	17	19	26	10
nlm	0	0	0	0	0	0

Table 2: L^2 error, number of iterations in the fixed point algorithm and percentage of local minima as a function of the discretization step for the VFPMMD scheme

h	$\frac{1}{8}$	$\frac{1}{16}$	$\frac{1}{32}$	$\frac{1}{64}$	$\frac{1}{128}$	$\frac{1}{256}$
L^2 error	2.8×10^{-2}	8.6×10^{-3}	1.8×10^{-3}	4.95×10^{-4}	7.7×10^{-5}	2×10^{-5}
nlm	0	0	1.7×10^{-1}	4.2×10^{-2}	1.0×10^{-2}	2.6×10^{-3}

Table 3: L^2 error and percentage of local minima as a function of the discretization step for the linear scheme

h	$\frac{1}{8}$	$\frac{1}{16}$	$\frac{1}{32}$	$\frac{1}{64}$	$\frac{1}{128}$	$\frac{1}{256}$
L^2 error	4.8×10^{-2}	1.05×10^{-2}	2.55×10^{-3}	5.9×10^{-4}	1.0×10^{-4}	3.0×10^{-5}
nlm	0	0	0	0	0	0

Table 4: L^2 error and percentage of local minima as a function of the discretization step for the VFPMMD scheme
(1 iteration)

3.2 Stationary solution using boundary conditions with steep gradients

To show the efficiency of the method, we consider test 3 described in [HER 08]. The computational domain is the square $]0,1.0[\times]0,1.0[$. We choose

$$\overline{\overline{D}} = R_\theta \begin{pmatrix} 1 & 0 \\ 0 & \delta \end{pmatrix} {R_\theta}^{-1}$$

where R_θ is the rotation of angle $\theta = 40$ degrees. The source term S is equal to zero. The Dirichlet boundary conditions are written as follows :

$$C = \begin{cases} 1 \text{ on } (0,.2) \times \{0.\} \cup \{0.\} \times (0,.2) \\ 0 \text{ on } (.8,1.) \times \{1.\} \cup \{1.\} \times (.8,.2) \\ \frac{1}{2} \text{ on } (.3,1.) \times \{0.\} \cup \{0.\} \times (.3,1.) \\ \frac{1}{2} \text{ on } (0.,0.7) \times \{1.\} \cup \{1.\} \times (0.,0.7) \end{cases}$$

Instead of a uniform rectangular mesh, we use 2 grids of triangular cells. The first is made up of 34 triangular cells and the second of about 9500 triangular cells. To test the robustness of our scheme, we set $\delta = 10^{-4}$. In this case, we expect to see more severe numerical oscillations. We show in Figures 5 through 8 the results obtained with the VFSYM scheme ([LP 05a]) and with the VFPMMD scheme. We observe oscillations on the linear scheme for the coarse and the fine grids. They disappear with the nonlinear scheme. On this problem, we only need 2 iterations in the fixed point algorithm to obtain minimum and maximum principles. To achieve convergence in the fixed point algorithm with the same criterion as in the previous section, we need 20 iterations for the coarse grid and 34 iterations for the fine grid. Note: if we take a uniform rectangular mesh, and $\delta = 10^{-3}$, no oscillations appear with the VFSYM scheme.

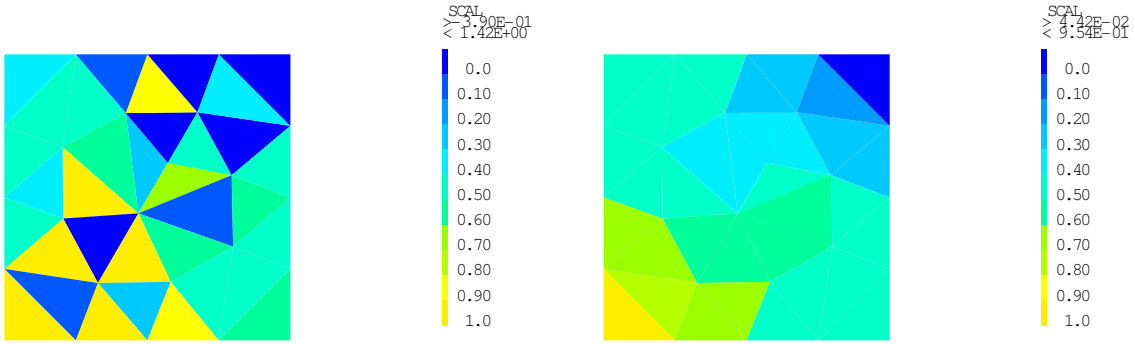

Figure 5: Concentration with VFSYM and VFPMMD schemes: 34 cells (for VFSYM scheme: maximum value 1.42, minimum value -0.39, for VFPMMD scheme: maximum value 0.954, minimum value 0.0442)

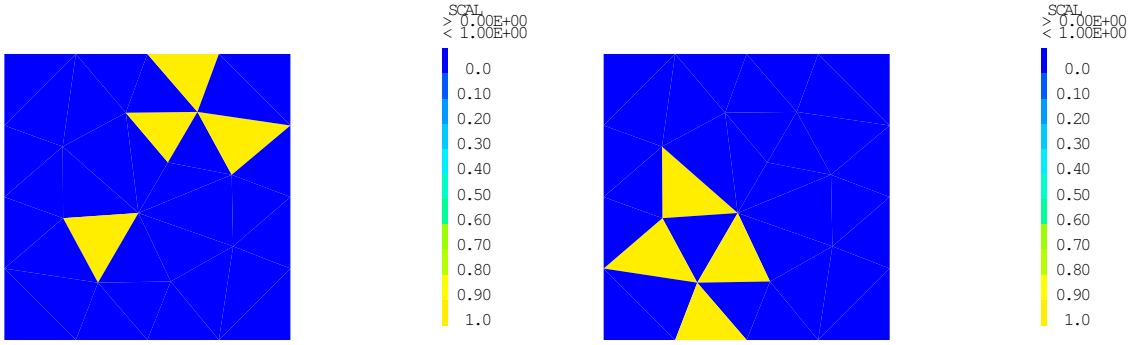

Figure 6: VFSYM scheme : in yellow, position of negative values (on the left) and values higher than 1 (on the right) ; 34 cells

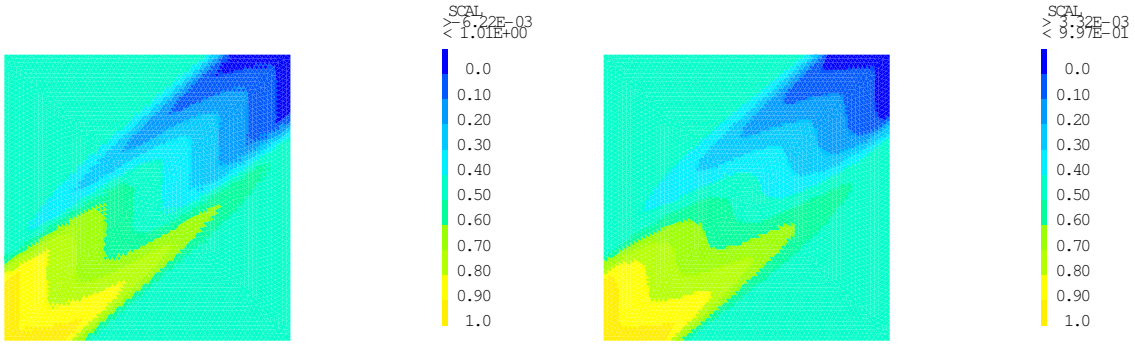

Figure 7: Concentration with VFSYM and VFPMMD schemes: 9500 cells, (for VFSYM scheme: maximum value 1.01, minimum value -6.22×10^{-3}, for VFPMMD scheme: maximum value 0.997, minimum value 3.32×10^{-3})

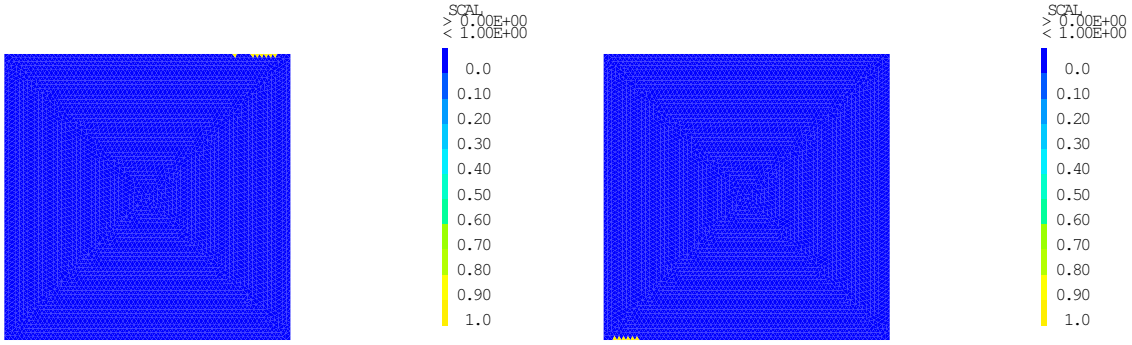

Figure 8: VFSYM scheme : in yellow, position of negative values (on the left) and values higher than 1 (on the right) ; 9500 cells

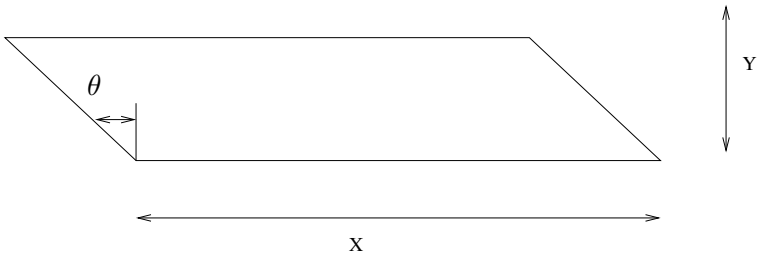

Figure 9: Parallelogram-shaped domain Ω showing the distances X, Y and θ

3.3 Stationary solution on perturbed parallelograms

This test is described in [HER 08] and is based on an idea of I. Aavsatmark. The domain Ω is parallelogram shaped. The parameters shown in figure 9 are $X = 1$, $Y = 1/30$ and $\theta = 30$ degrees. The medium is homogeneous and isotropic with $\overline{\overline{D}} = Id$. The grid is made up of perturbed parallelogram meshes. The boundary conditions and right hand side S satisfy :

$$\begin{cases} S = 0 \text{ all cells except cell}(6,6) \text{ where } \int_{\text{cell}(6,6)} \text{S(x)dx} = 1 \\ C = 0 \ on \ \partial\Omega \end{cases} \tag{23}$$

For the VFPMMD scheme, we divide each quadrangular cell into two triangular cells. We show in Figures 10 the results obtained with the VFSYM scheme and with the VFPMMD scheme. With the first algorithm, we observe large oscillations. With the second method, we check that the solution remains positive and has no local minima. With the same criterion as in the previous section in the fixed point algorithm, the positivity is obtained for 212 iterations and the convergence is achieved for 238 iterations.

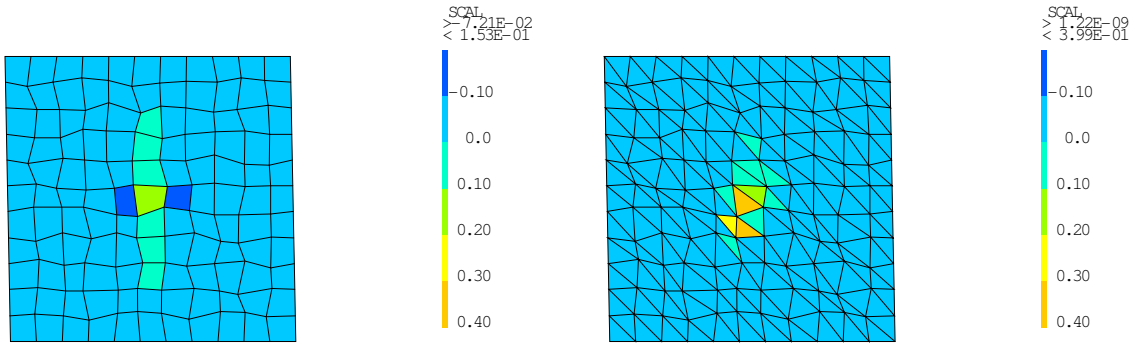

Figure 10: Concentration with VFSYM and VFPMMD schemes: perturbed parallelograms

3.4 Anisotropy and wells

This example is test 9 described in [HER 08]. The domain Ω is a square unit domain. The grid is a square uniform grid with 11×11 cells. The medium is homogeneous and anisotropic with $\overline{\overline{D}} = R_\theta \begin{pmatrix} 1 & 0 \\ 0 & 10^{-3} \end{pmatrix} {R_\theta}^{-1}$, R_θ is the rotation of angle $\theta = 67.5$ degrees. The source term S is equal to zero. The boundary conditions are homogeneous Neumann conditions at the outer boundary : $\overline{\overline{D}}\vec{\nabla}C \cdot \vec{n} = 0$. The pressure is fixed in two cells of the grid : $C = 0$ in cell (4,6) and $C = 1$ in cell (8,6). For the VFPMMD scheme, we divide each quadrangular cell into two triangular cells. We show in Figures 11 the results obtained with the VFSYM scheme and with the VFPMMD scheme. With the first algorithm, we observe large oscillations. With the second method, we check that the solution remains between 0 and 1. The solution becomes inferior to 1 for 46 iterations and the positivity is obtained for 85 iterations. With the same criterion as in the previous section in the fixed point algorithm, the convergence is achieved for 191 iterations.

4 Conclusion

We have shown the efficiency and the robustness of the new scheme for anisotropic heterogeneous diffusion. Our scheme has the key property that we obtain a global matrix which is a strictly diagonally dominant M-Matrix. However, this matrix depends on the solution and so the scheme is nonlinear. The VFPMMD scheme satisfies, simultaneously, minimum and maximum principles. We have shown that the oscillations which can be present in non-monotone linear methods disappear with our algorithm. We emphasize that this scheme is particularly interesting in the case where the transport model is coupled with nonlinear chemical models. Indeed, in this case, it is, of course, very important to calculate positive chemical element concentrations.

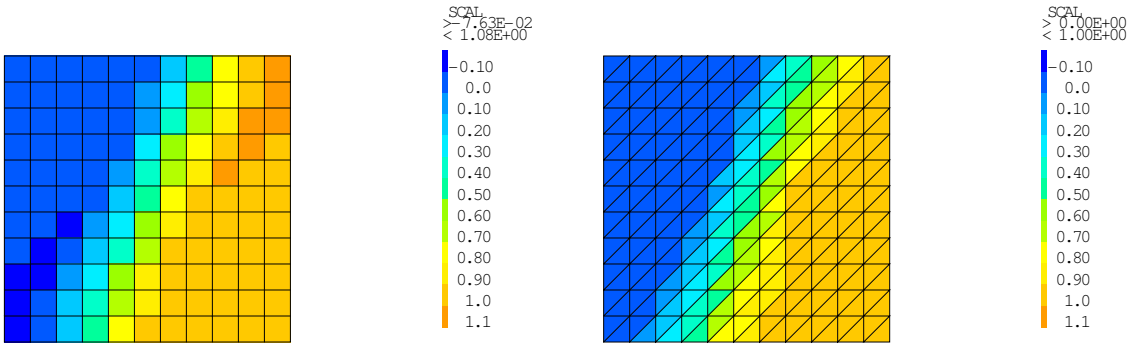

Figure 11: Concentration with VFSYM and VFPMMD schemes: anisotropy and wells

Acknowledgments

The author would like to thank gratefully Donna Calhoun for remarks and comments.

References

[BER 06] Bertolazzi E., Manzini G., a second-order maximum principle preserving volume method for steady convection-diffusion problems, SIAM Journal on Numerical Analysis, 43(5): 2172-2199 (2006)

[BUR 04] Burman E., Ern A., Discrete maximum principle for Galerkin approximations of the Laplace operator on arbitrary meshes, Comptes Rendus Mathematique, Volume 338, Issue 8, 15 April 2004, Pages 641-646

[COU 99] Coudière Y., Analyse de schémas volumes finis sur maillage non structurés pour des problèmes linéaires hyperboliques et elliptiques. Thèse de l'université Paul Sabatier de Toulouse, 1999

[CIA 73] Ciarlet P.G., Raviart P.A., Maximum principle and uniform convergence for the finite element method, Comput. Methods Appl. Mech. Engrg. 2 (1973) 17-31.

[EYM 99] Eymard R., Gallouët T., Herbin R., Finite Volume Method, Handbook of Numerical Analysis, Vol VII, 2000. Editors: P.G. Ciarlet and J.L. Lions (1999)

[HER 08] Herbin. R., Hubert F., Benchmark on Discretization Schemes for Anisotropic Diffusion Problems on General Grids, Finite Volumes for Complex Applications V, R. Eymard and J.-M. Herard eds, Wiley, 2008, pp. 659-692

[GAL 06] Gallouët T., Personnal communication at VF06: Anisotropie à Porquerolles

[KAP 07] Kapyrin I, A family of monotone methods for the numerical of three-dimensional diffusion problems on unstructured tetrahedral meshes, Dokl. Math. 2007, Vol. 76, n^0 2, pp. 734-738

[KOR 00] Korotov S., Křížek M., Neittaanmäki, Weakened acute type condition for tetrahedral triangulations and the discrete maximum principle, Math. Comp. 70(233) (2000) 107-119

[LP 05a] Le Potier C., Schéma volumes finis pour des opérateurs de diffusion fortement anisotropes sur des maillages non structurés, C. R. Acad. Sci., Ser. I 340 (2005) 921-926

[LP 05b] Le Potier C., Schéma volumes finis monotone pour des opérateurs de diffusion fortement anisotropes sur des maillages de triangles non structurés, C. R. Acad. Sci., Ser. I 341 (2005) 787-792

[LP 09] Le Potier C., Un schéma linéaire vérifiant le principe du maximum pour des opérateurs de diffusion très anisotropes sur des maillages déformés, C. R. Acad. Sci., Ser. I 347 (2009) 105-110

[LIP 07] Lipnikov K., Shashkov M., Svyatskiy D., Vassilevski Yu., Monotone finite volume schemes for diffusion equations on unstructured triangular and shape-regular polygonal meshes, Journal of Computational Physics 227 (2007) 492-512

[LIP 09] Lipnikov K., Svyatskiy D., Vassilevski Yu., Interpolation-free monotone finite volume method for diffusion equations on polygonal meshes, Journal of Computational Physics 228 (2009) 703-716

[NOR 05] Nordbotten J.M., Aavastsmark I., Eigestad G.T., Monotonicity of control volume methods, Numerische Mathematik, 106:255-288, 2007.

[YUA 08] Yuan G., Sheng Z., Monotone finite volume schemes for diffusion equations on polygonal meshes, Journal of Computational Physics 227 (2008) 6288-6312